Diffraction Of Water Waves By A Submerged Circular Cylinder

by

Hin Chiu

University of California

University of California
Institute of Marine Resources
P.O. Box 1529
La Jolla, California 92037

University of California, Berkeley
College of Engineering Report No. NA-73-4
UC-IMR Reference No. 74-2
Sea Grant Publication No. 5

DIFFRACTION OF WATER WAVES BY A SUBMERGED CIRCULAR CYLINDER

by

Hin Chiu

This work is a result of research sponsored by NOAA Office of Sea Grant, Department of Commerce, under Grant # USDC 2-35208. The U.S. Government is authorized to produce and distribute reprints for governmental purposes, notwithstanding any copyright notation that may appear hereon.

July 1973

Available from:
University of California
Institute of Marine Resources
P.O. Box 1529
La Jolla, California 92037

University of California, Berkeley
College of Engineering Report No. NA-73-4

UC-IMR Reference No. 74-2
Sea Grant Publication No. 5

TABLE OF CONTENTS

ACKNOWLEDGEMENT

The author wishes to express his appreciation to Professor J. R. Paulling, Jr. and Professor J. V. Wehausen for their guidance and support on this project. Work was done in conjunction with Dr. Paulling's Sea Grant project, R/E-4, "Synthesis of Forces on Marine Structures." Thanks also go to Professor T. Francis Ogilvie, Department of Naval ARchitecture and Marine Engineering, University of Michigan, for the release of his numerical computations. Finally, special thanks should be given to Mr. O. J. Sibul for his help in the experiment.

NOMENCLATURE

A_I = Incident-wave amplitude.

A_R = Reflected-wave amplitude.

H_I = Incident-wave height.

H_T = Transmitted-wave height.

λ = Wave length.

K, k = Wave number $= 2\pi/\lambda$.

σ = Circular frequency ($2\pi/T$).

ϵ = Wave slope (for incident waves).

c = Group velocity.

h = Submergence of cylinder center to mean water surface.

d = Mean water depth.

a = Radius of cylinder.

$E_{av(T)}$ = Average energy flux per unit width of the transmitted waves through a fixed plane perpendicular to the direction of wave propagation.

$E_{av(I)}$ = Average energy flux per unit width of the incident waves through a fixed plane perpendicular to the direction of wave propagation.

$\mathcal{F}$ = Force function.

η = Wave profile.

Φ = Velocity potential.

F_k = Exciting force ($k = x, y$).

T = Wave period.

I. INTRODUCTION

In this paper, we shall discuss the physical phenomenon which occurs when a train of regular harmonic waves passes over a submerged circular cylinder. This problem was first solved by Dean (1948). He introduced a complex potential function which satisfied the Laplace equation and the appropriate linearized boundary conditions. By conformal mapping, the flow field inside the bounding surfaces was mapped onto an annulus where the potential function could be expressed by a Laurent series. After solving for the coefficients of the Laurent series in a special case, he obtained the conclusion that, in general, the coefficient of reflection is zero, and at a great distance from the cylinder, there is a phase angle between the incident and transmitted waves, while the amplitude remains the same.

Ursell (1950) obtained the same conclusion as Dean by a different approach and included a uniqueness proof. In his work, a system of multipoles is placed at the center of the cylinder. The oscillation was expressed by a symmetric and an antisymmetric part of a velocity distribution, each of which satisfied all boundary conditions. He gave the following solution for the velocity potential when the cylinder was fixed in the fluid:

$$\Phi = \frac{g A_I}{\sigma} \exp(-Ky)\cdot\cos(Kx+\sigma t) + \Phi_1$$

$$\Phi_1 \to 0 \qquad \text{as} \quad x \to +\infty$$

$$\Phi_1 \to -4\pi a \exp(-K(y+h))\left[\sin(Kx+\sigma t)\cdot\sum_{r=1}^{\infty}\frac{P_r}{r!} - \cos(Kx-\sigma t)\cdot\sum_{r=1}^{\infty}\frac{g_r}{r!}(Ka)^r\right]$$

$$\text{as} \quad x \to -\infty$$

where y is positive downward.

The approximate determination of p_r and q_r in the above expression involved a finite set of linear equations.

Ogilvie (1963) gave a numerical solution of the exciting forces for a cylinder fixed in the fluid by applying Ursell's procedure. The solution is expressed as a series in a perturbation parameter. The results from the linearized (first-order) theory show that the first-order forces in the horizontal and vertical directions are equal in magnitude, but that there exists a phase angle of 90 degrees between them. The second-order horizontal force vanished, while in the vertical direction there was a constant suction directed against gravity.

Here we report an experimental study of this problem. A discrepancy between the theoretical and experimental results is found when the cylinder is close to the water surface, as one might expect. A discussion of this will appear in the later sections.

II. FORMULATION OF THE PROBLEM

The two-dimensional problem will be treated here. The fluid is assumed inviscid, incompressible, and irrotational. These assumptions imply that there exists a velocity potential Φ which satisfies the Laplace equation:

$$\Phi_{xx} + \Phi_{yy} = 0$$

The velocity potential must also satisfy the following boundary conditions:

1) $\Phi_x \eta_x - \Phi_y = \eta_t$ on the free surface $y = \eta(x,t)$.

2) $\Phi_t + g\eta + \frac{1}{2}(\Phi_x^2 + \Phi_y^2) = 0$ on the free surface .

3) $\Phi_n\big|_S = 0$ on the cylinder surface S .

4) $\Phi_y(x, -d, t) = 0$ for finite depth.

$\lim_{y\to\infty} \Phi_y = 0$ for infinite depth.

5) The radiation condition: The waves must be outgoing at a great distance from the cylinder.

The Exciting Forces

The exciting forces can be evaluated by integrating the pressure distribution around the cylinder surface,

$$F_k = \int_0^{2\pi} p \cdot \cos(n,k)\, a\, d\theta \qquad k = x, y$$

where p can be obtained from Euler's integral:

$$p + \rho g y + \frac{1}{2}\rho(\Phi_x^2 + \Phi_y^2) + \rho \Phi_t = 0$$

The Wave Profile

The exact formulation for the surface-wave profile can be expressed as follow:

$$\eta(x,t) = -\frac{1}{g}\left[\Phi_t(x,\eta) + \frac{1}{2}\left(\Phi_x^2(x,\eta) + \Phi_y^2(x,\eta)\right)\right]$$

However, there are difficulties in solving the above equation since η is imbedded in the function Φ .

The approximate solution can be obtained by a perturbation method. The parameter ϵ in the series expansion might be chosen equal to the incident wave slope. The first-order and second-order wave profile are given by:

$$\eta^{(1)} = -\frac{1}{g}\,\Phi_t^{(1)}(x,0,t)$$

$$\eta^{(2)} = -\frac{1}{g}\left[\Phi_t^{(2)} + \eta^{(1)}\,\Phi_{ty}^{(1)} + \frac{1}{2}\left(\Phi_x^{(1)2} + \Phi_y^{(1)2}\right)\right]$$

III. THE TECHNIQUE OF WAVE MEASUREMENT

1) The Testing Tank

The experiment was carried out in the Ship Model Towing Tank, Department of Naval Architecture, at the University of California, Berkeley. The tank measures 200 feet long, 8 feet wide, 6 feet deep and has a rectangular cross-section. The wave generator is of the bulkhead type. It makes waves between 2.4 ft. and 40 ft. in length. The wave amplitude can be varied from 0 to 8 inches. There is a wave damper at the end of the tank. The reflection of the waves is less than 4 percent if the wave period is less than one second.

2) The Measurement of Reflected Waves

It is assumed that there exists a reflection from the cylinder even though theory predicts the reflection to vanish. Consider the incident wave η_I and reflected wave η_R :

$$\eta_I = A_I \cos(Kx - \sigma t)$$

$$\eta_R = A_R \cos(Kx + \sigma t + \beta_R)$$

The origin of the coordinate system is set on the mean surface level above the center of the cylinder. Then $\eta_I + \eta_R$ consists of a superposition of progressive and standing waves. They can be expressed in the following form:

$$\eta_I + \eta_R = (A_I - A_R) \sin(Kx + \tfrac{1}{2}\beta_R) \sin(\sigma t + \tfrac{1}{2}\beta_R) +$$

$$+ (A_I + A_R) \cos(Kx + \tfrac{1}{2}\beta_R) \cos(\sigma t + \tfrac{1}{2}\beta_R)$$

At a point where $\sin(Kx + \frac{1}{2}\beta_R) = 1$, $\cos(Kx + \frac{1}{2}\beta_R) = 0$ this gives $(A_I - A_R)\sin(\sigma t + \frac{1}{2}\beta_R)$. At a point where $\sin(Kx + \frac{1}{2}\beta_R) = 0$, $\cos(Kx + \frac{1}{2}\beta_R) = 1$ which gives $(A_I + A_R)\cos(\sigma t + \frac{1}{2}\beta_R)$. This allows one to determine A_I and A_R by moving a wave probe against the incoming waves in order to find the envelope. Any effect of reflection from the far end of the tank has been neglected in the above analysis.

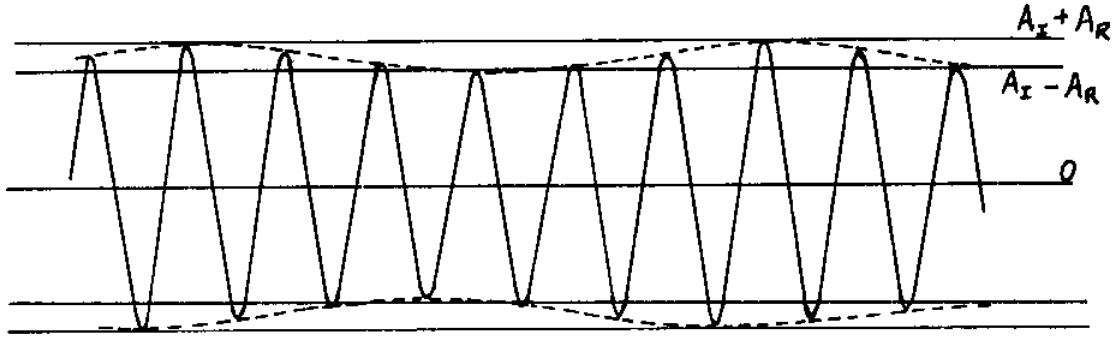

THE ENVELOPE

The determination of the phase angle between the incident wave and reflected wave can be done in several ways. Since the experimental results showed that A_R is almost zero, computation of β_R was not attempted.

3) <u>The Wave-Probe Arrangement</u>

There were three wave probes designed to measure the incident waves, the envelope, and the transmitted waves, respectively.

No. 1 probe, 60 feet in front of the cylinder was used to measure the incident waves. These waves are used only for reference.

No. 2 probe, mounted on the carriage, was designed to move slowly against the incident waves in the region between the No. 1 probe and the cylinder. It measured the envelope formed by reflected and incident waves.

No. 3 probe, designed to measure the transmitted waves, was placed a distance greater than 30 feet behind the cylinder. At this distance the local disturbance will have decayed to a negligible value.

The distance between the No. 1 probe and No. 3 probe was adjusted to an integral number of incident wave lengths in each test case so that the phase could be compared directly in the output.

The cylinder was fixed at 90 feet from the wave-maker. The signals from the wave probes and the force gages (described in the next section) were amplified and displayed simultaneously on one chart in five channels. Two dimensionless parameters were chosen in the experiment. They are Ka and h/a. The parameter Ka governed the change in the wave lengths. The submergence factor h/a governed the changes in the depth of submergence. The range of these two parameters is as follows:

$$0.135 \leq Ka \leq 0.86$$

(corresponding to $15.5\,ft \geq \lambda \geq 2.44\,ft$),

$$1.275 \leq h/a \leq 13.0$$

(corresponding to $0.425\,ft \leq h \leq 4.33\,ft$).

The water depth at rest was 5.25 feet. The minimum and maximum incident-wave amplitude in the experiment was equal to 0.297 inches and 0.572 inches, respectively, corresponding to the wave length λ = 2.49 feet and λ = 15.49 feet.

IV. THE DESIGN OF THE DYNAMOMETER

1) Model and Strain Gages

The model was made of an aluminum tube, 8 feet long, 8 inches outside diameter, and 1/8 inch wall thickness. It was divided into three sections. The 14 inch long center test section was designed to be watertight. A flexible plastic membrane covered the clearance between the center and end sections. A total of 19 lbs of ballast had been placed symmetrically in the test section to keep it neutrally buoyant in the submerged condition. A rigid steel box beam passes through the center section. This beam is bolted to two end sections [see Figures 1 and 2].

For the force-gage arrangement, there are two vertical elements and one horizontal element. The bottoms of the vertical elements were screwed onto an aluminum support which connected to the inner wall of the cylinder. One end of the horizontal element was fixed to the steel box beam while the other end was connected to the top of the vertical elements by a solid aluminum block. The arrangement is shown in Figure 3.

Since the forces act through the center of the cylinder cross-section, consider now that a vertical force is acting on the cylinder. This force is transmitted

from the vertical element to the horizontal element. In this case, the vertical elements are acting like a column under compression on an elastic support and the horizontal element is acting like a beam under combined flexure and pure bending. The loading diagram and bending-moment diagram of the horizontal element may be shown as follows:

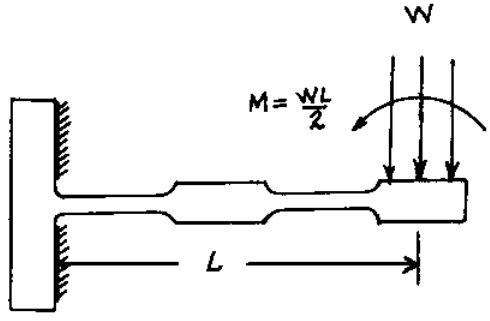

LOADING DIAGRAM

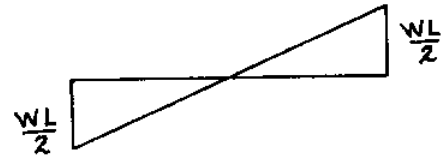

BENDING-MOMENT DIAGRAM

The magnitudes of the strains are equal on both ends of the horizontal element, so that four bonded strain gages can be placed on the opposite faces at each end and connected to form a Wheatstone bridge. The direct strains on the vertical elements caused by these vertical forces are negligible.

The same loading condition will appear on the vertical elements for the horizontal-force measurement.

The maximum designed load on the test section is in either direction $\pm$7.0 lbs., with a safety factor equal to 3 in the static condition. The strength of the gages is great enough for testing in random waves. (Testing in random waves will not be discussed in this paper.)

2) Calibration of the Gages

The calibration was carried out statically. The cylinder was fixed under the water surface transversely across the tank. Both horizontal and vertical loadings were applied to the center of the test section by means of weights, strings, and pulleys. The strains were found to be linear with respect to the test loadings.

The cross-coupling effect between horizontal and vertical sensitivity was found to be within 3 percent. The value is negligible as far as the purpose of the experiment is concerned.

The sensitivity of the gages was such that they had a minimum sensitivity (least count) of ± 0.05 lbs. of loading.

V. DATA ANALYSIS

1) The Reflected Waves

The reflection coefficients, defined as the ratio of reflected-wave and incident-wave amplitude, are shown in Figure 4. It shows that the maximum value of the reflection coefficient never exceeds 0.07, but also that no matter how deep the submergence of the cylinder, there still exists a small reflection. This reflection may mainly come from the end of the tank.

2) Transmitted Waves

A. Shallow-submergence condition (h/a = 1.275 and h/a = 1.50)

Each of the transmitted-wave patterns measured from the No. 3 wave probe is plotted for one cycle as shown in Figure 5. These patterns are periodic in time. In fact, one may get two different patterns at two different positions, but their spectra should be identical. A Fourier analysis of the wave patterns has been made in the following form:

$$F(t) = C_o + \sum_{n=1}^{16} A_n \sin(n\sigma t) + \sum_{n=1}^{16} B_n \cos(n\sigma t)$$

The spectra, plotted as $A_T^2/A_I^2 \equiv (A_n^2 + B_n^2)/A_I^2$ are shown in Figures 6 to 8. The white spectra are for h/a equal to 1.275, the black spectra are for h/a equal to 1.50.

Since the transmitted waves are not pure sinusoids, it is meaningless to get the transmission coefficient by comparing their amplitudes to the incident-wave amplitudes. Instead, a comparison of the transmitted energy has been used. The flux of the energy per unit width through a fixed plane perpendicular to the direction of wave propagation is given, according to the linearized theory for the incident wave, by

$$E(x,t) = \rho c \int_{-d}^{0} \Phi_{I,x}^2(x, y, t)\, dy$$

where Φ_I is the velocity potential of the incident waves and c is the group velocity. The average energy flux over one period is given by:

$$E_{av} = \frac{1}{4} \rho g A_I^2 c \left[1 + \frac{2Kd}{\sinh(2Kd)} \right]$$

$$\approx \frac{1}{4} \rho g^{3/2} A_I^2 K^{-1/2}$$

By superposition, the average energy flux per unit width through a fixed plane across the transmitted waves is given, with reference to the Fourier expansion, by

$$E_{av(T)} = \frac{1}{4} \rho g^{3/2} K^{-1/2} \left[(A_1^2 + B_1^2) + \frac{(A_2^2+B_2^2)}{\sqrt{2}} + \frac{(A_3^2 + B_3^2)}{\sqrt{3}} + \cdots \right]$$

The energy transmission coefficient, defined as $E_{av(T)}/E_{av(I)}$, is plotted against Ka in Figure 9b. From the figure, one can see that the energy transmission coefficients are always less than one, as one expects. In addition, there is a hollow at $Ka = 0.4$ and a hump at $Ka = 0.6$.

One important effect must be pointed out here, that is, the energy transmission coefficient not only depends on the incident-wave number and the depth of submergence of the cylinder, but also depends on the incident-wave slope. This effect has been tested in the special case where $Ka = 0.602$, $h/a = 1.275$ were fixed. The only variable parameter was the incident-wave slope ε. The result showed that the energy transmission coefficient was equal to 0.85 for $\varepsilon = 0.0459$ and equal to 0.93 for $\varepsilon = 0.0663$. At the same time, the transmitted-wave pattern measured at a fixed position has also changed. These are plotted below:

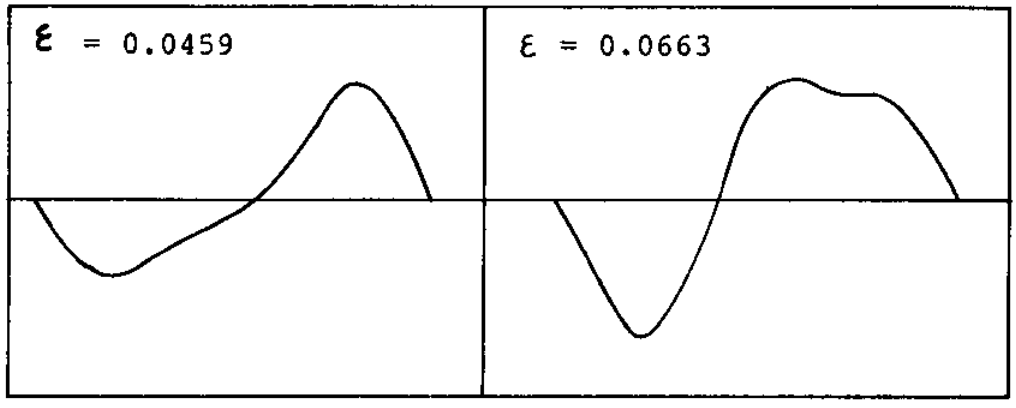

B. Moderately Submerged Condition ($h/a = 2$, $h/a = 3$)

In this condition, the transmitted waves became sinusoidal in shape. The transmission coefficient is taken as the ratio of the height of the transmitted wave and incident wave. Their values are somewhat higher than those in the shallow-submergence condition. The hump and hollow still exists in the curve of the transmission coefficient.

C. Deep-Submergence Condition ($h/a > 5$)

In this condition, the hump and hollow in the curve of the transmission coefficient disappeared. In general, the transmission coefficient is higher than 0.95.

D. Long Waves ($Ka \leq 0.2$)

It is found that in all cases with $Ka \leq 0.2$ the transmission coefficient is practically unity. This may be explained by the fact that the wave slopes were so

small ($\varepsilon < 0.025$) that the linearized theory gives a good prediction of the behavior. There is also the possibility that the superposition of reflected waves from the end of the tank and the transmitted waves might have enlarged the measured values of the apparent transmitted-wave amplitude.

E. The Phase Angle

Both experimental and first-order theoretical results indicated a large variation of the phase angle between the incident waves and transmitted waves when the cylinder was close to the water surface. In such a case, neither result is accurate enough. The inaccuracy of the experimental result is due to the reflection of the tank. The inaccuracy of the first-order linearized solution is due to neglecting the nonlinear effect of the finite wave height. A test at moderate submergence has been carried out to test the effect of wave slope. In the test, the wave number was fixed at $K = 1.22$ and the submergence factor h/a was fixed at 3.0. The incident-wave slope was given four different values: $\varepsilon_1 = 0.0282$, $\varepsilon_2 = 0.0429$, $\varepsilon_3 = 0.0613$, $\varepsilon_4 = 0.0795$. The corresponding phase angles were $\psi_1 = 73°$, $\psi_2 = 67°$, $\psi_3 = 60°$, $\psi_4 = -30°$, respectively. The sudden change of phase angle at $\varepsilon = 0.0795$ may have been caused by a nonlinear effect. However, in the same test, the increment of the exciting force was found almost to be linear in the wave slope.

3) The Exciting Forces

In Figure 13, there are displayed the measured exciting forces and the first-order theoretical solution.

The force function shown in the figure is defined by:

$$|F_k| = \frac{2\pi\rho g A_I}{K} \cdot \mathcal{F}$$

For deep-water waves, $Ka > 0.2$, $2Kh > 0.4$, all forces displayed in the chart have the appearance of a sinusoidal function. The 90 degree phase shift between the vertical and horizontal forces is verified. The theoretical prediction stating that the exciting force decreases exponentially with the depth of submergence is also verified.

For long waves, for example at $Ka = 0.135$, where the ratio of the wave length to the mean water depth is equal to 2.95, there exists a bottom effect. No matter how deep the submergence of the cylinder was, the exciting forces are no longer sinusoidal.

There is a good agreement, in general, between the experimental and theoretical results. Only in one condition, at $h/a = 1.275$, did the experimental curves deviate significantly from the theoretical solution. The order of magnitude of the measured horizontal and vertical forces is the same except in one case. That is, at $Ka = 0.4$, $h/a = 1.275$, $\varepsilon = 0.044$, the case corresponding to the "hollow" in the energy-transmission curve. There the horizontal-force amplitude is 1.27 times larger than the vertical-force amplitude.

In shallow submergence, $h/a = 1.275$ and $h/a = 1.50$, there is a horizontal drift force that varied from 0 percent to 47 percent of the horizontal-force amplitude as Ka

decreased from 0.6 to 0.135 and ε decreased from 0.058 to 0.0194. A second-order vertical suction appeared at $h/a = 1.275$. Their values are plotted in Figure 16. In all other conditions, this second-order force was so small that its value was out of the range of the sensitivity of the strain gages.

VI. CONCLUSIONS

1) The linearized potential theory gives a good description of the phenomenon in case the cylinder is well submerged.

2) The phase angle between the incident waves and transmitted waves is found to be very sensitive with respect to the change of incident-wave slope. This effect may be related to the change of the proportion of the energy propagation that passed over the top and below the cylinder. A further study of this effect is needed.

3) For the transmitted-wave profile, the solution should be extended to second-order when the submergence factor (h/a) is less than 2.

4) The exciting-force measurements were in satisfactory agreement with the theoretical solution. The viscous effect seems negligible for the geometry studied here.

5) The reflection coefficient was found to be very small. One might consider that a submerged cylinder with minimum reflection coefficient is of circular cross-section.

REFERENCES

1) W. R. Dean

On the reflection of surface waves by submerged circular cylinder. Proc. Cambridge Philos. Soc. 44 (1948), pp. 483-491.

2) F. Ursell

Surface waves on deep water in the presence of a submerged circular cylinder. I & II. Proc. Cambridge Philos. Soc. 46 (1950), pp. 141-158.

3) T. Francis Ogilvie

First- and second-order forces on a cylinder submerged under a free surface. J. Fluid Mechanics 16 (1963), pp. 451-472.

4) J. N. Newman

Diffraction of water waves. Applied Mechanics Reviews, January (1972)

5) J. V. Wehausen; Laitone, E. V.

Surface waves. Encyclopedia of Physics, vol. IX, pp. 446-778. Springer-Verlag, Berlin, 1960.

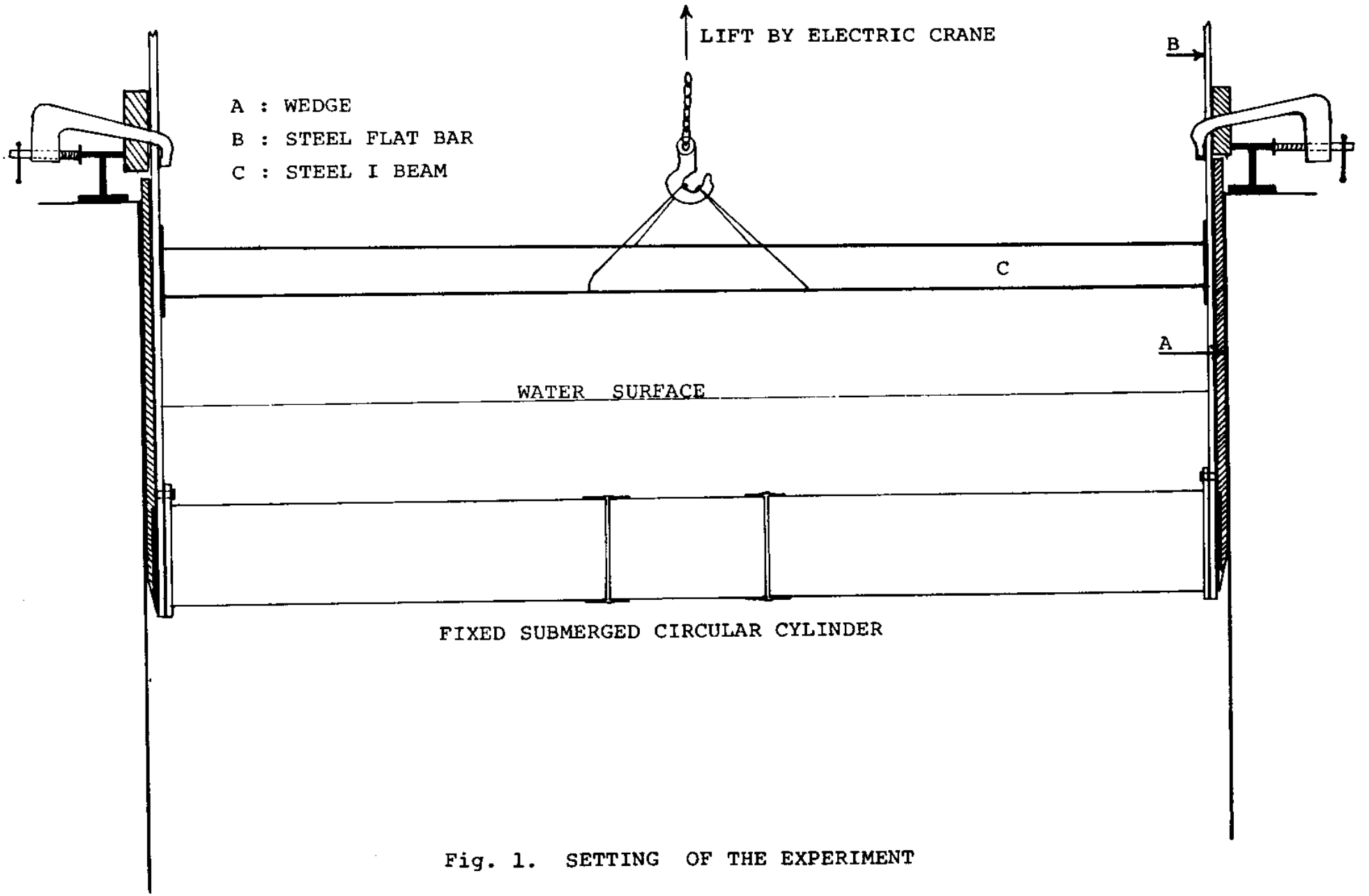

Fig. 1. SETTING OF THE EXPERIMENT

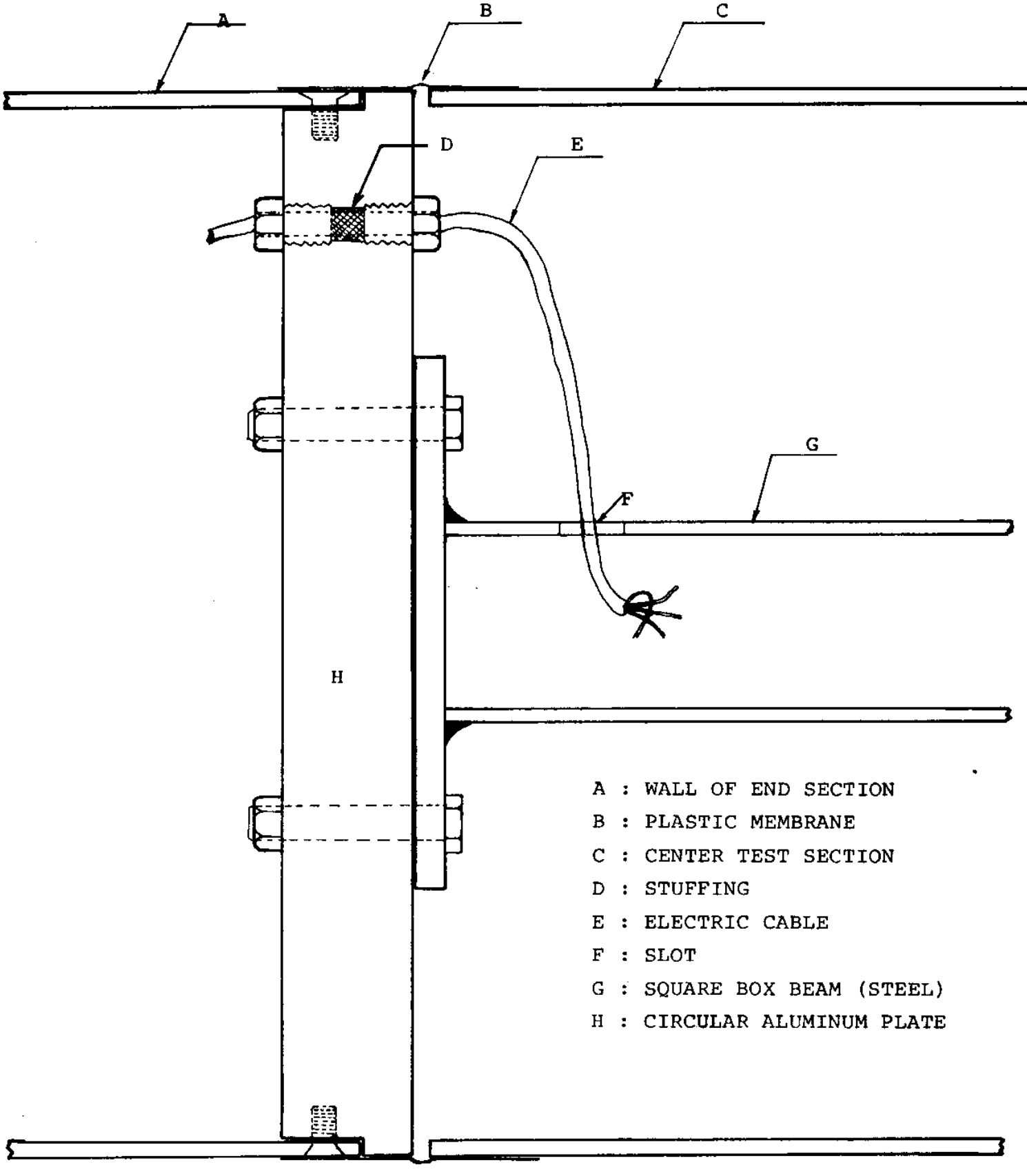

Fig. 2. DESIGN OF WATERTIGHT TEST SECTION

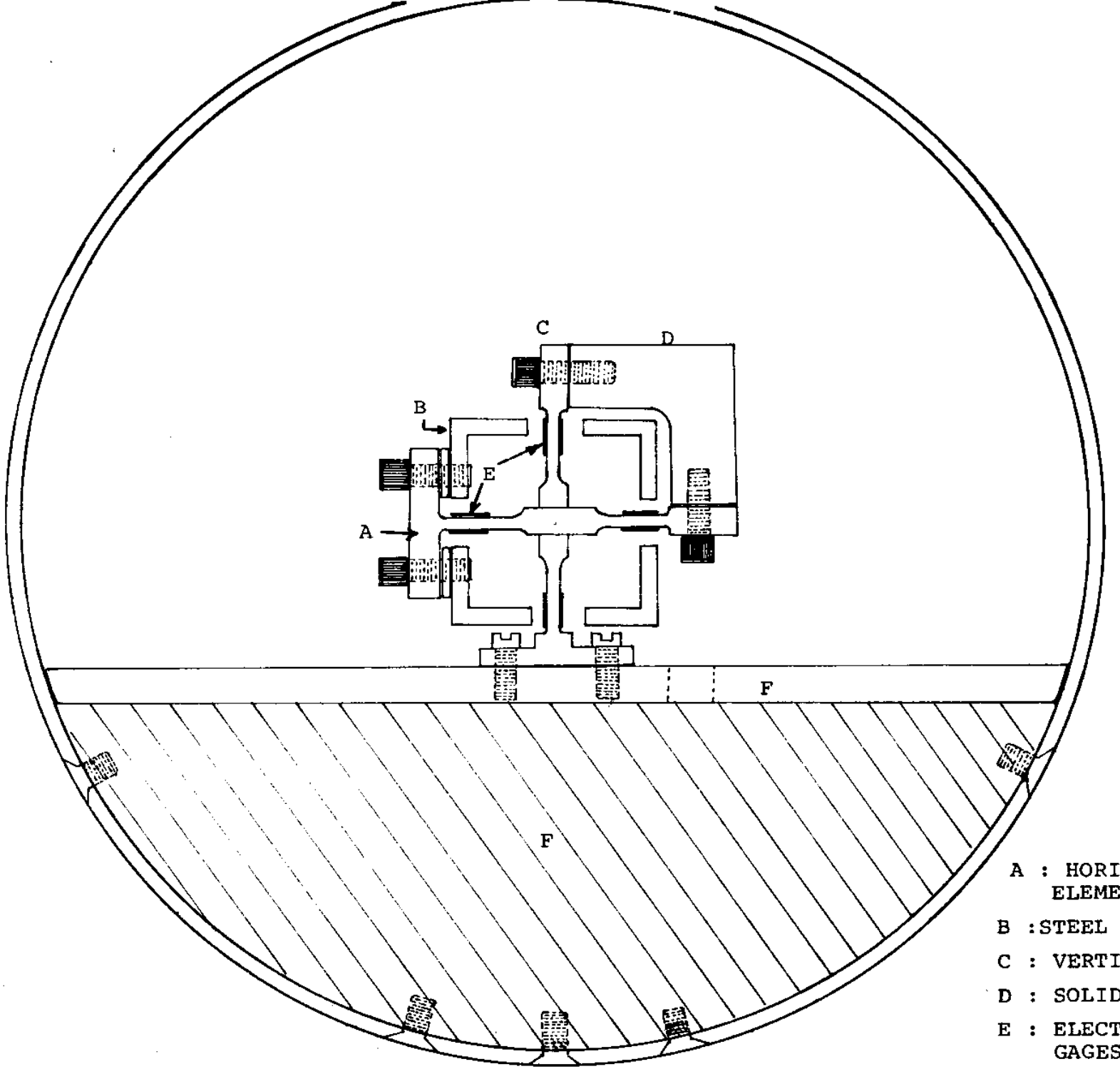

A : HORIZONTAL ELEMENT.

B : STEEL BOX BEAM

C : VERTICAL ELEMENT

D : SOLID AL. BLOCK

E : ELECTRIC STRAIN GAGES.

F : ALUMINUM PLATE

Fig. 3. STRAIN GAGE ARRANGEMENT

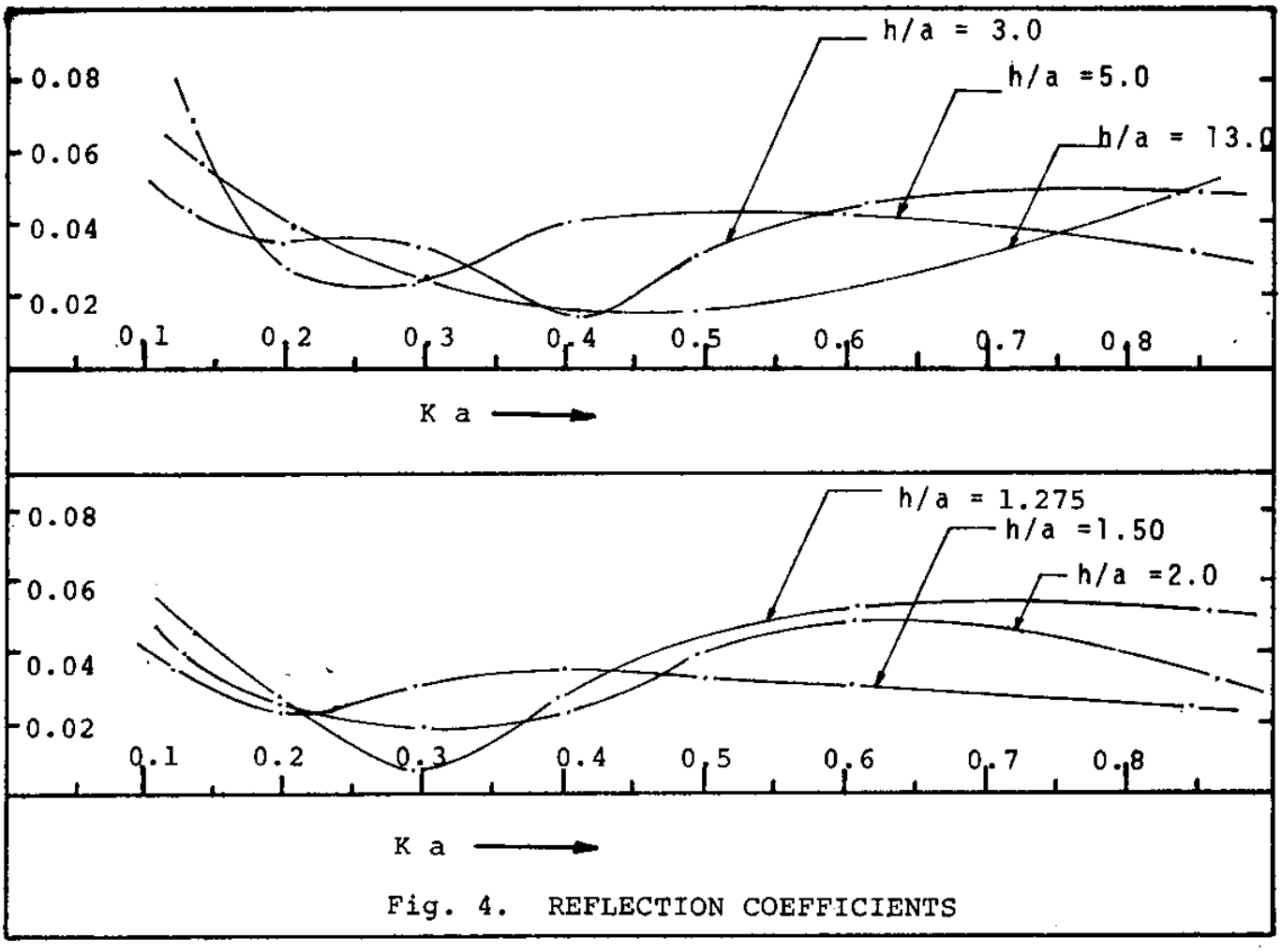

Fig. 4. REFLECTION COEFFICIENTS

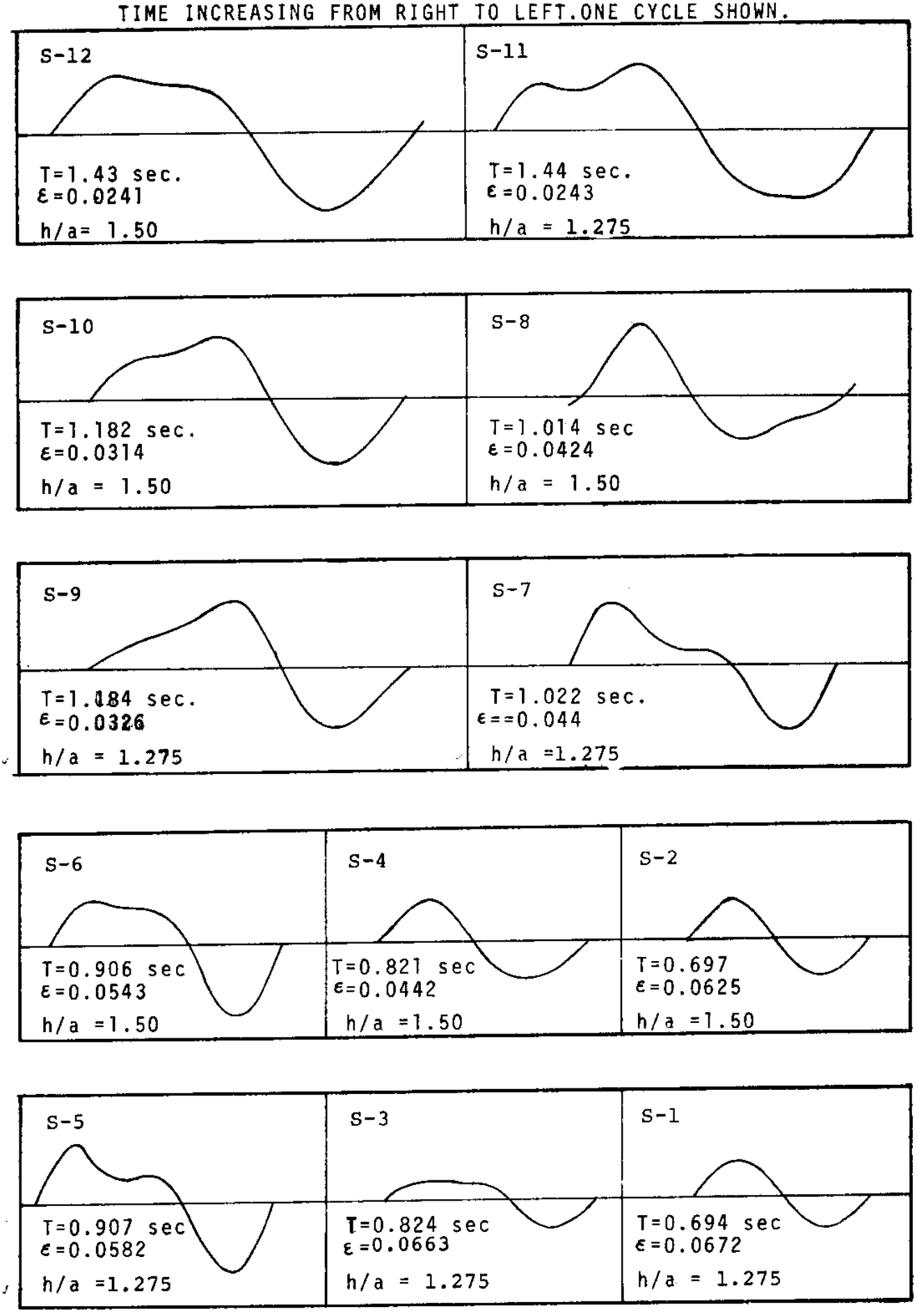

Fig. 5. TRANSMITTED-WAVE PATTERNS (ONE CYCLE)

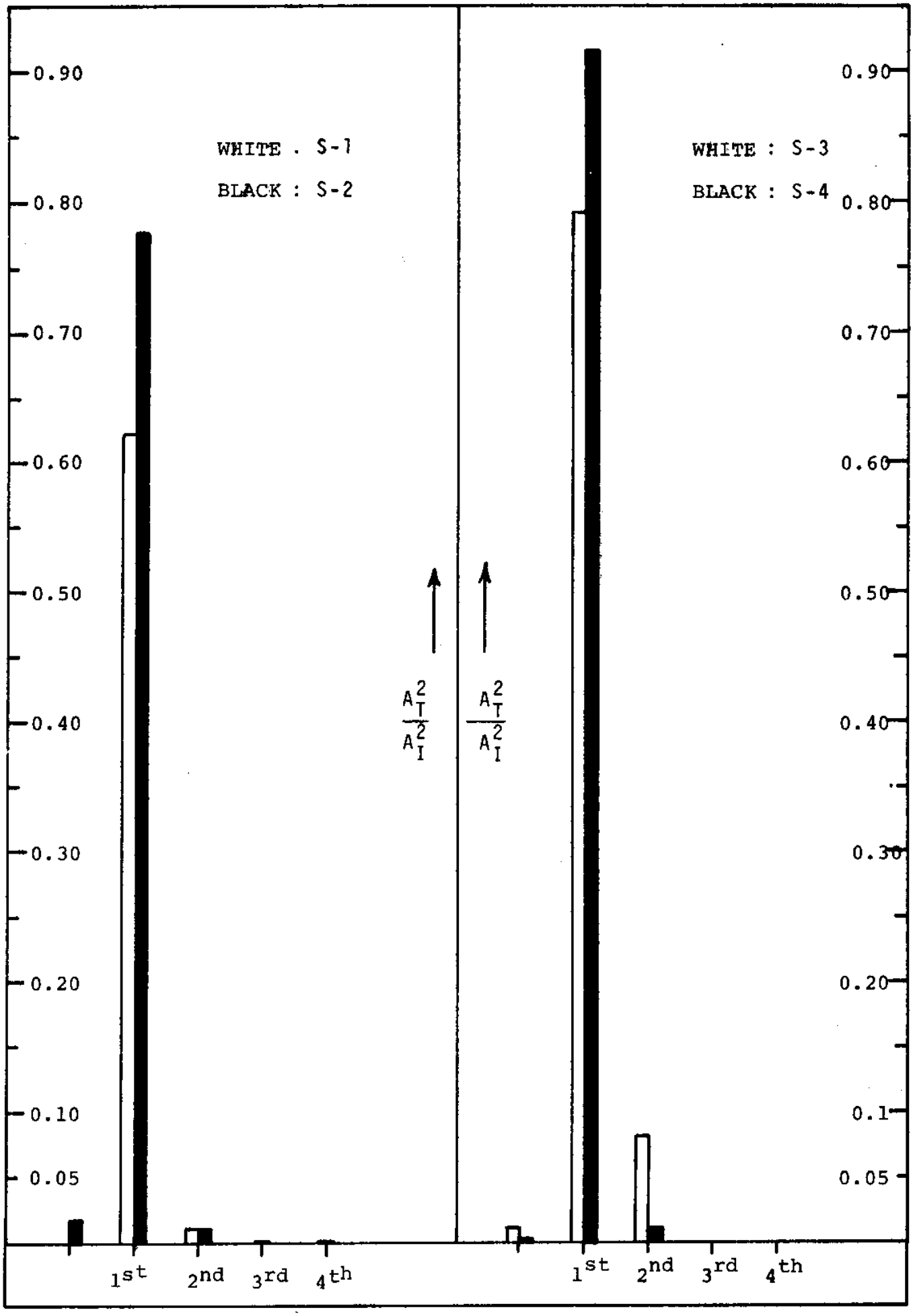

Fig. 6. SPECTRUM OF TRANSMITTED WAVES

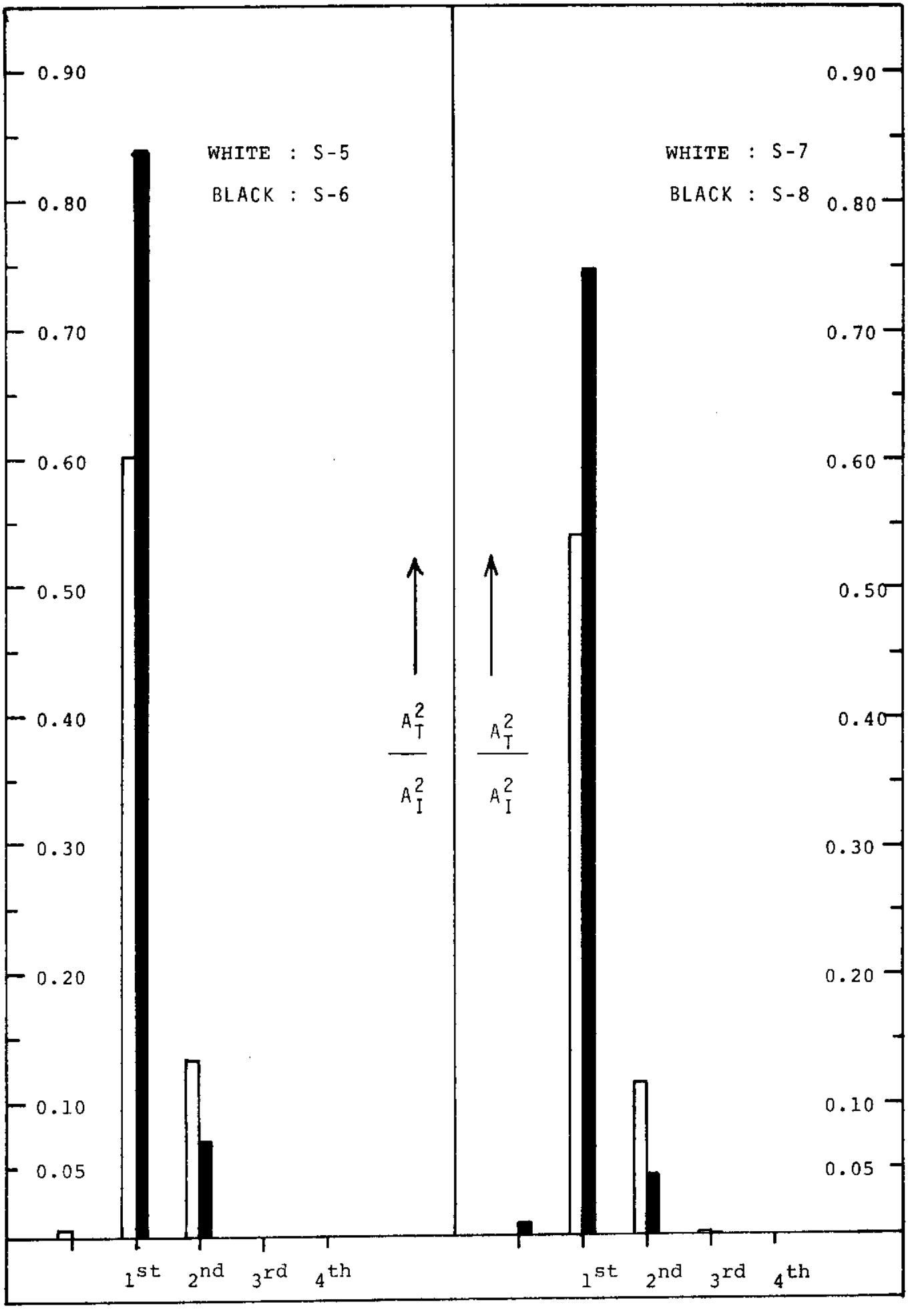

Fig. 7. SPECTRUM OF TRANSMITTED WAVES

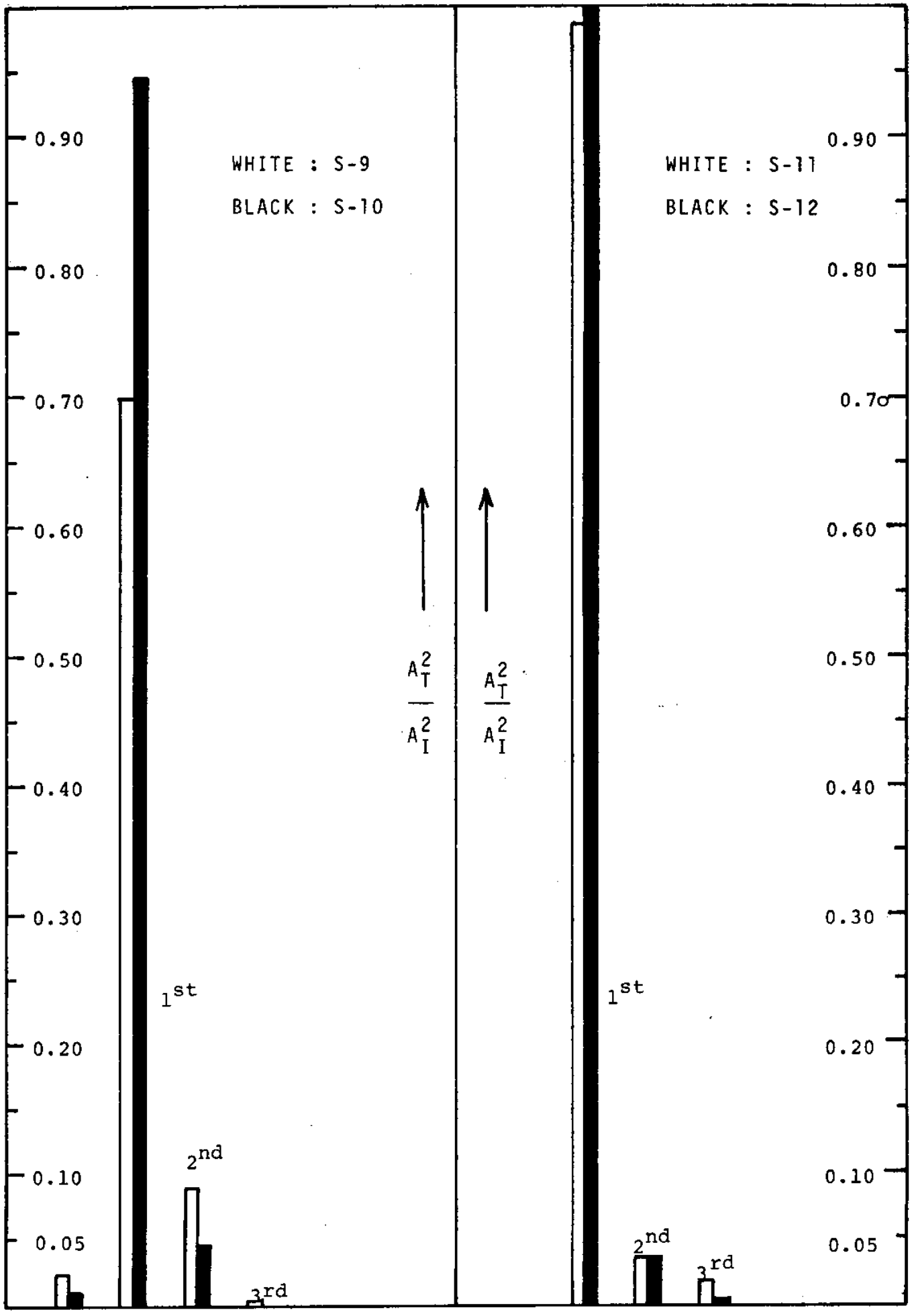

Fig. 8. SPECTRUM OF TRANSMITTED WAVES

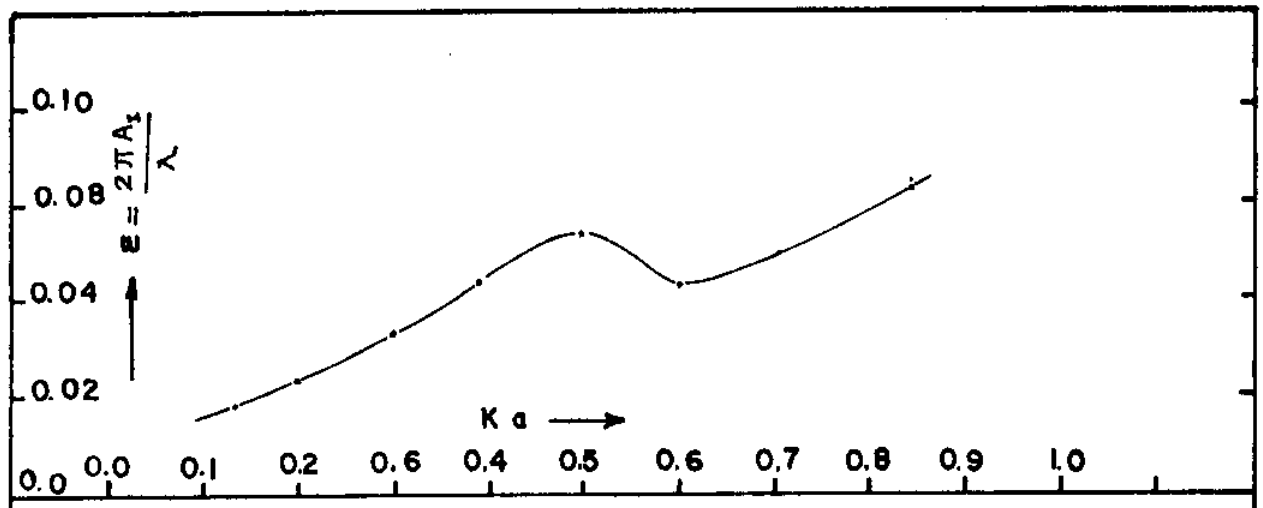

FIG. 9a

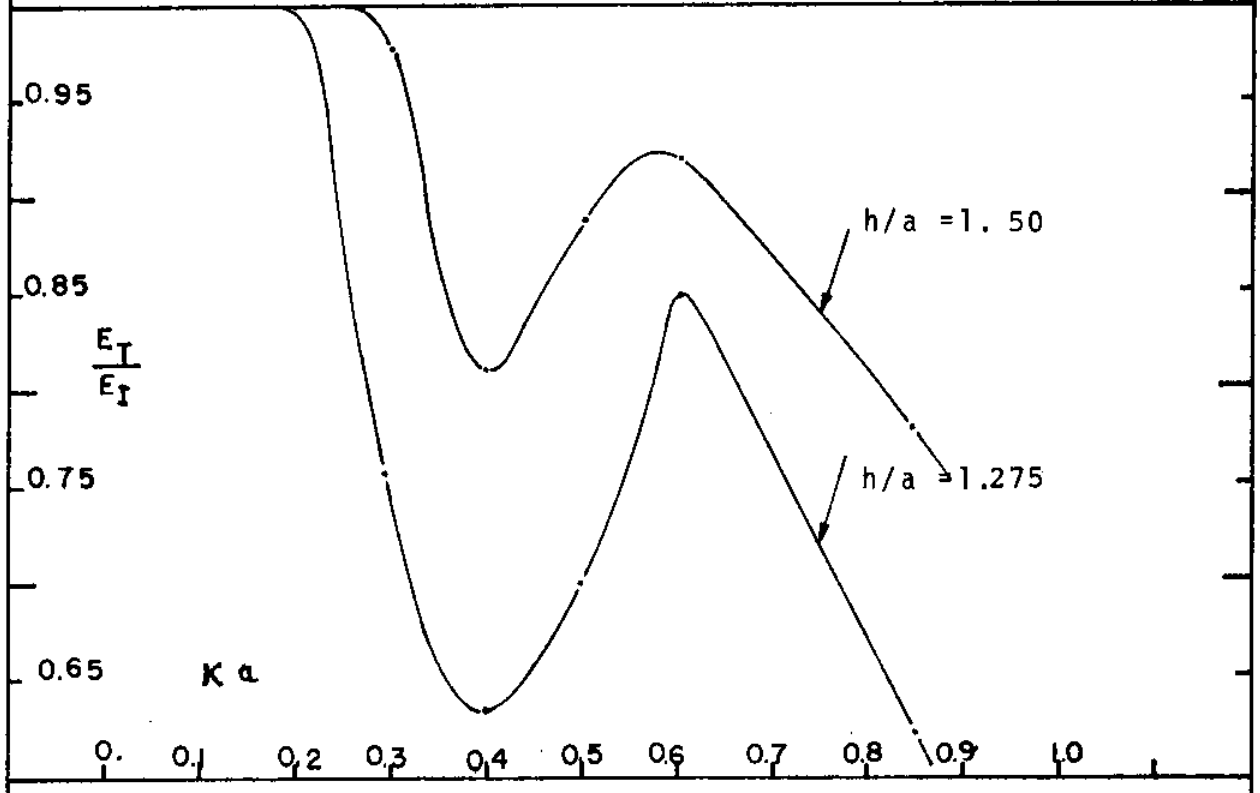

Fig. 9b. ENERGY TRANSMISSION COEFFICIENTS

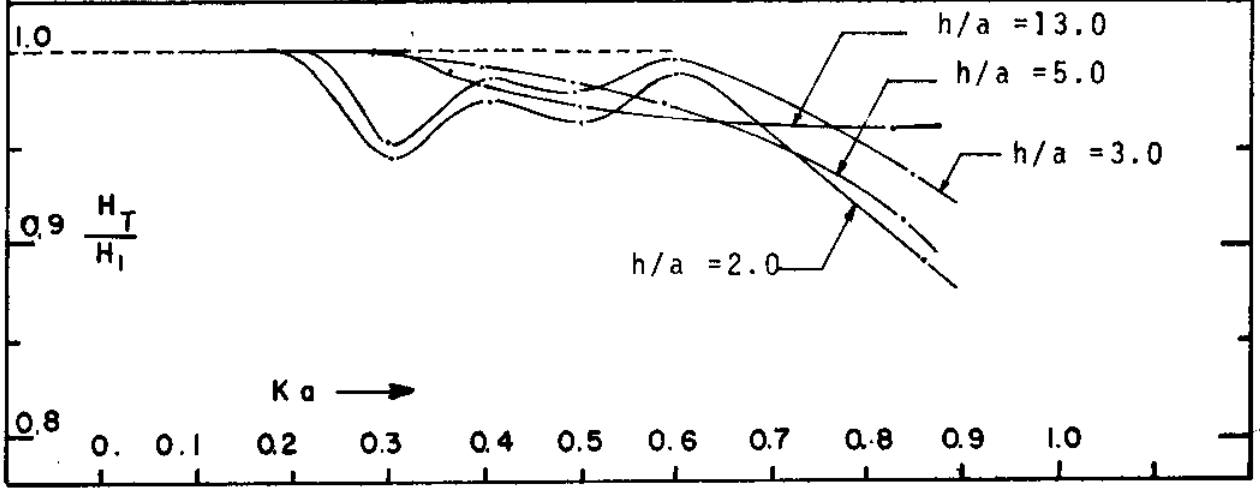

Fig. 10. TRANSMISSION COEFFICIENTS

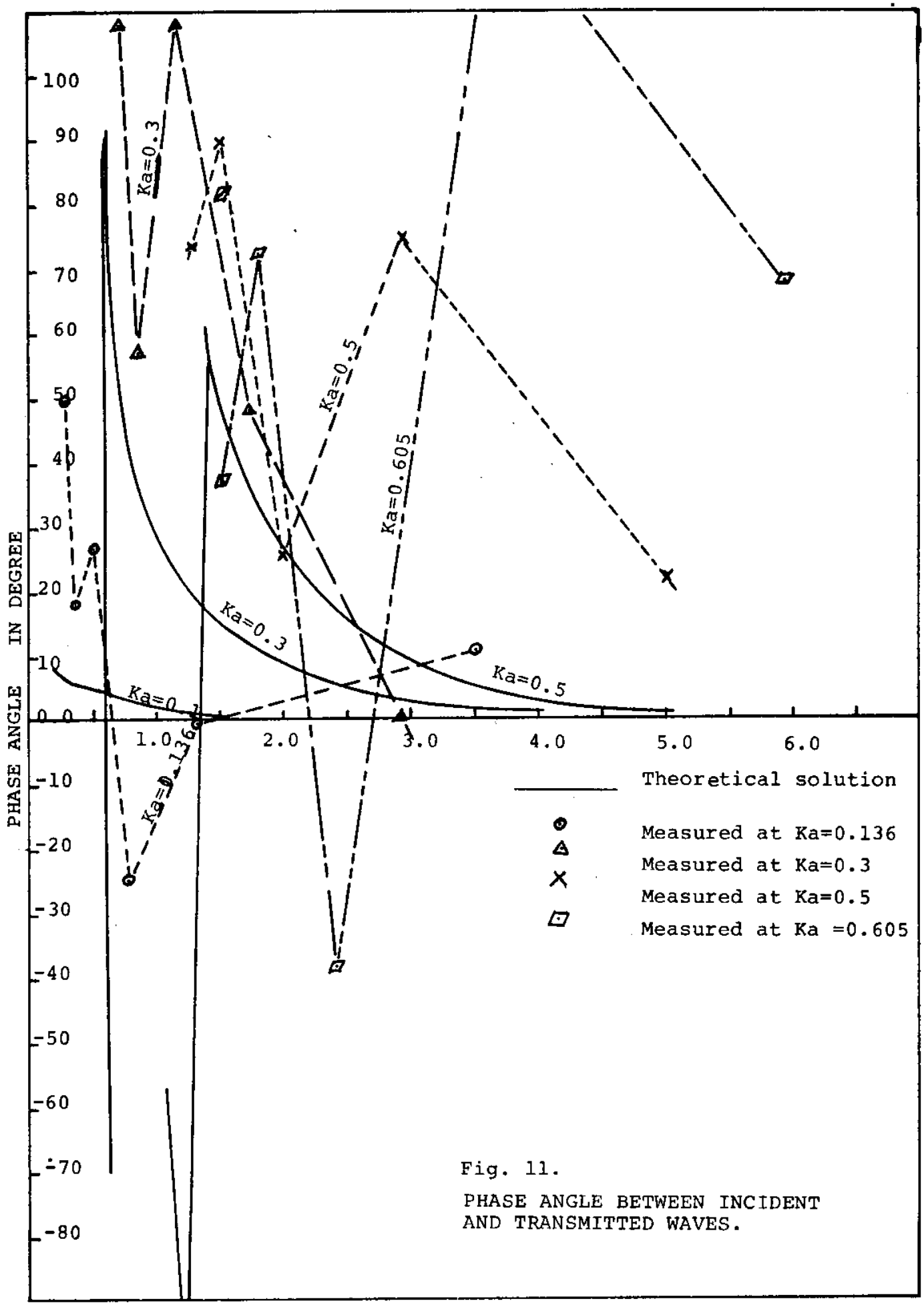

Fig. 11.

PHASE ANGLE BETWEEN INCIDENT AND TRANSMITTED WAVES.

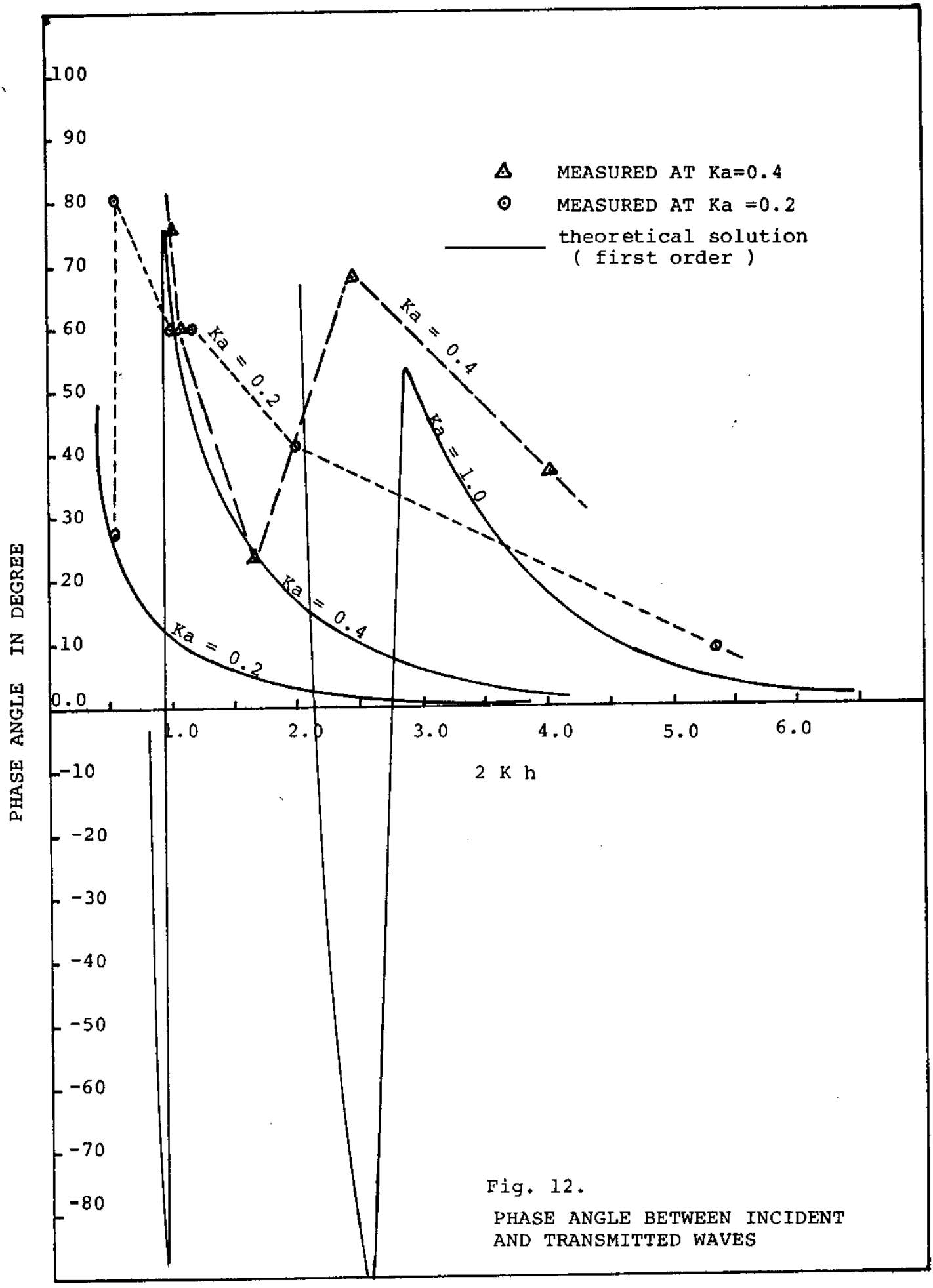

Fig. 12.

PHASE ANGLE BETWEEN INCIDENT AND TRANSMITTED WAVES

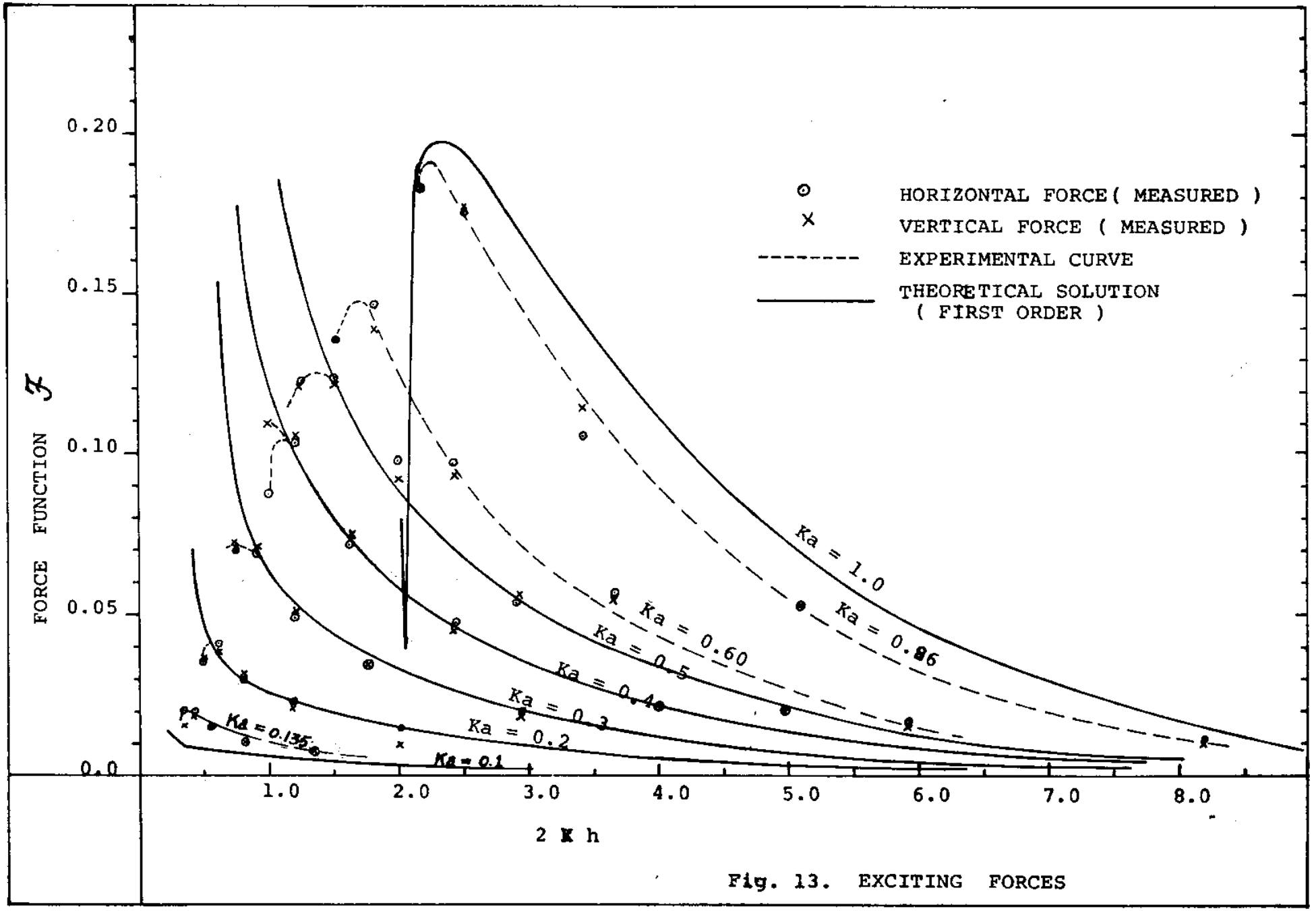

Fig. 13. EXCITING FORCES

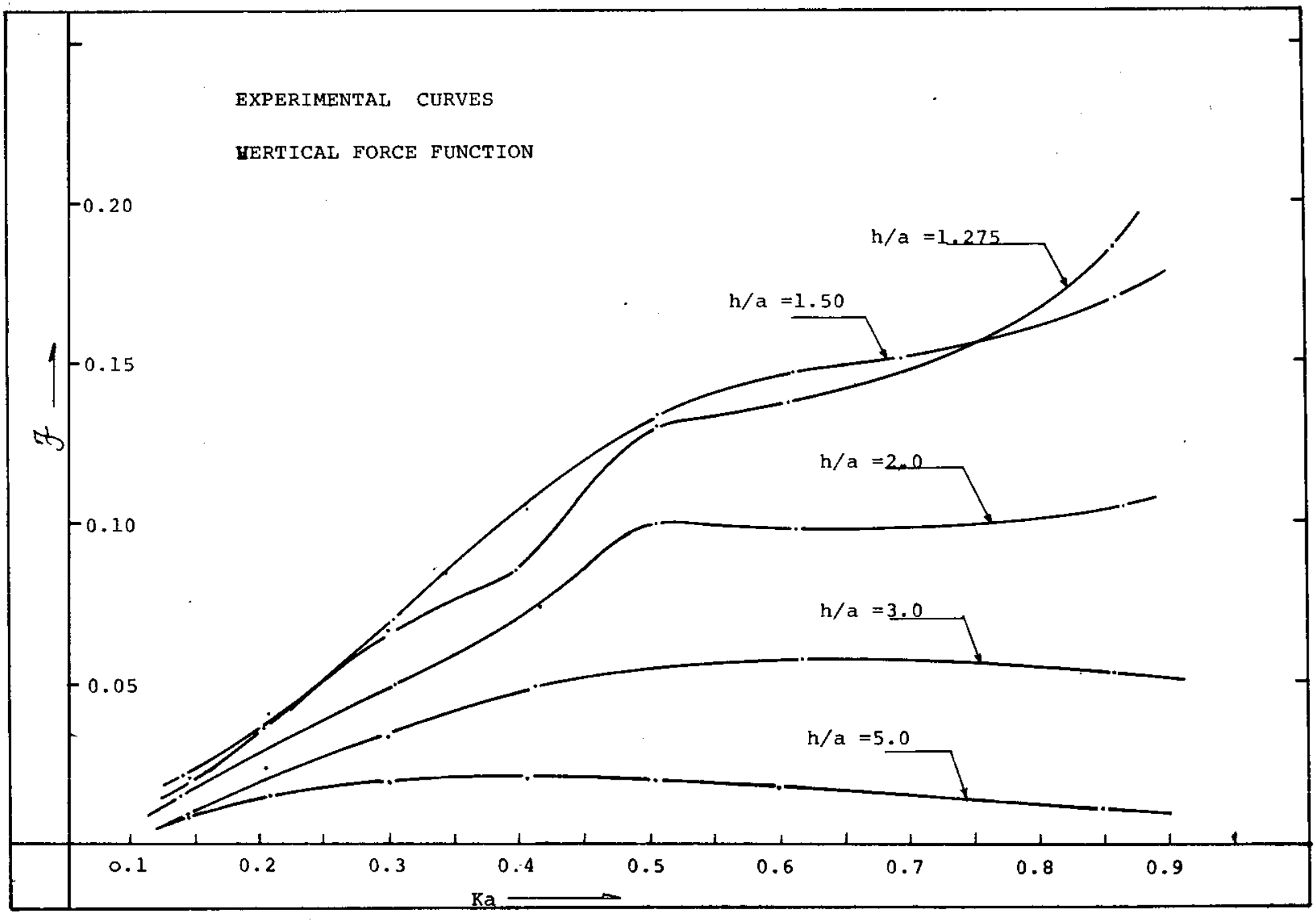
EXPERIMENTAL CURVES
VERTICAL FORCE FUNCTION
0.20
0.15
0.10
0.05
f
h/a =1.275
h/a =1.50
h/a =2.0
h/a =3.0
h/a =5.0
0.1
0.2
0.3
0.4
0.5
0.6
0.7
0.8
0.9
Ka

Fig. 14

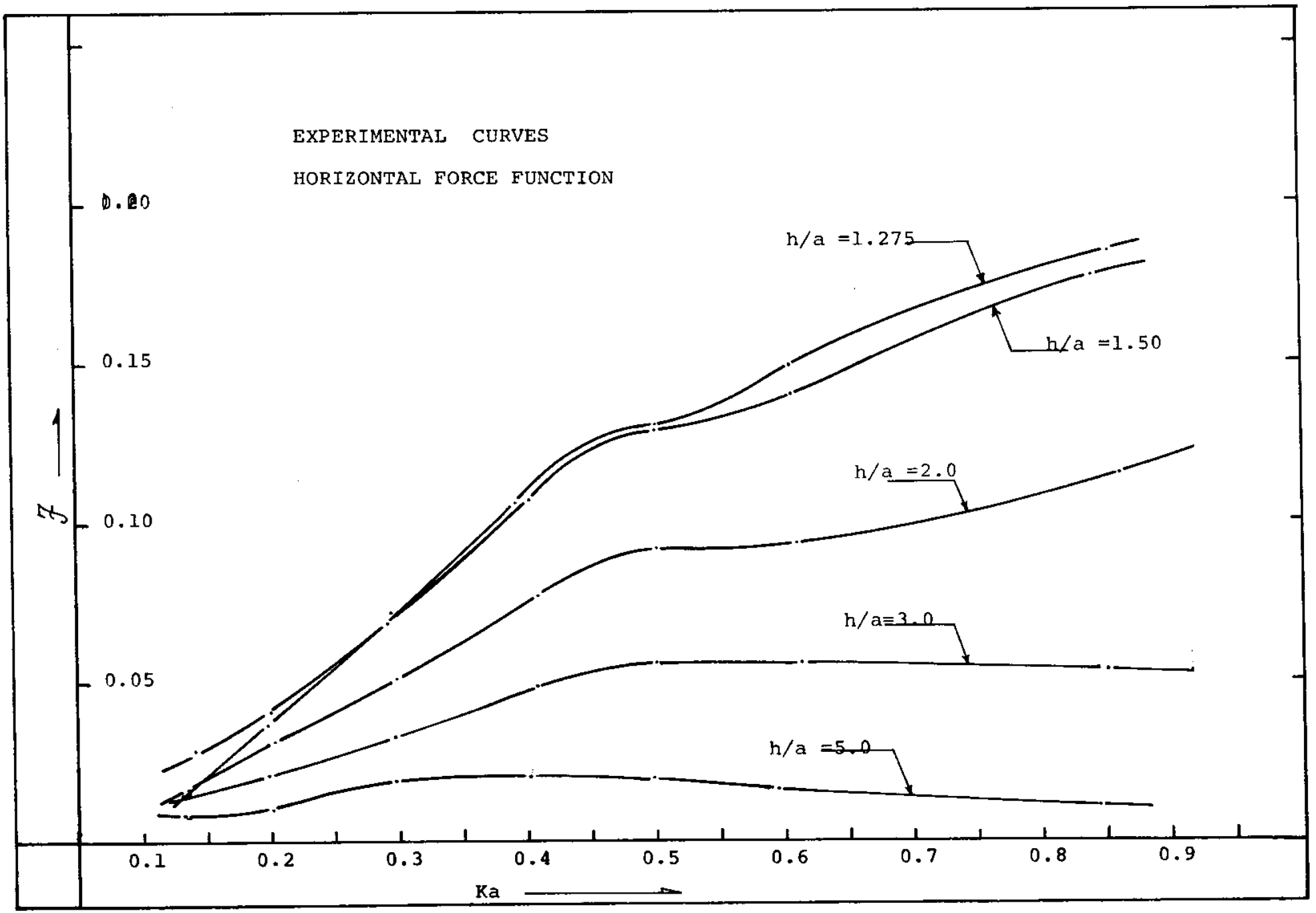
EXPERIMENTAL CURVES
HORIZONTAL FORCE FUNCTION
0.20
0.15
0.10
0.05
f
h/a =1.275
h/a =1.50
h/a =2.0
h/a=3.0
h/a =5.0
0.1
0.2
0.3
0.4
0.5
0.6
0.7
0.8
0.9
Ka

Fig. 15

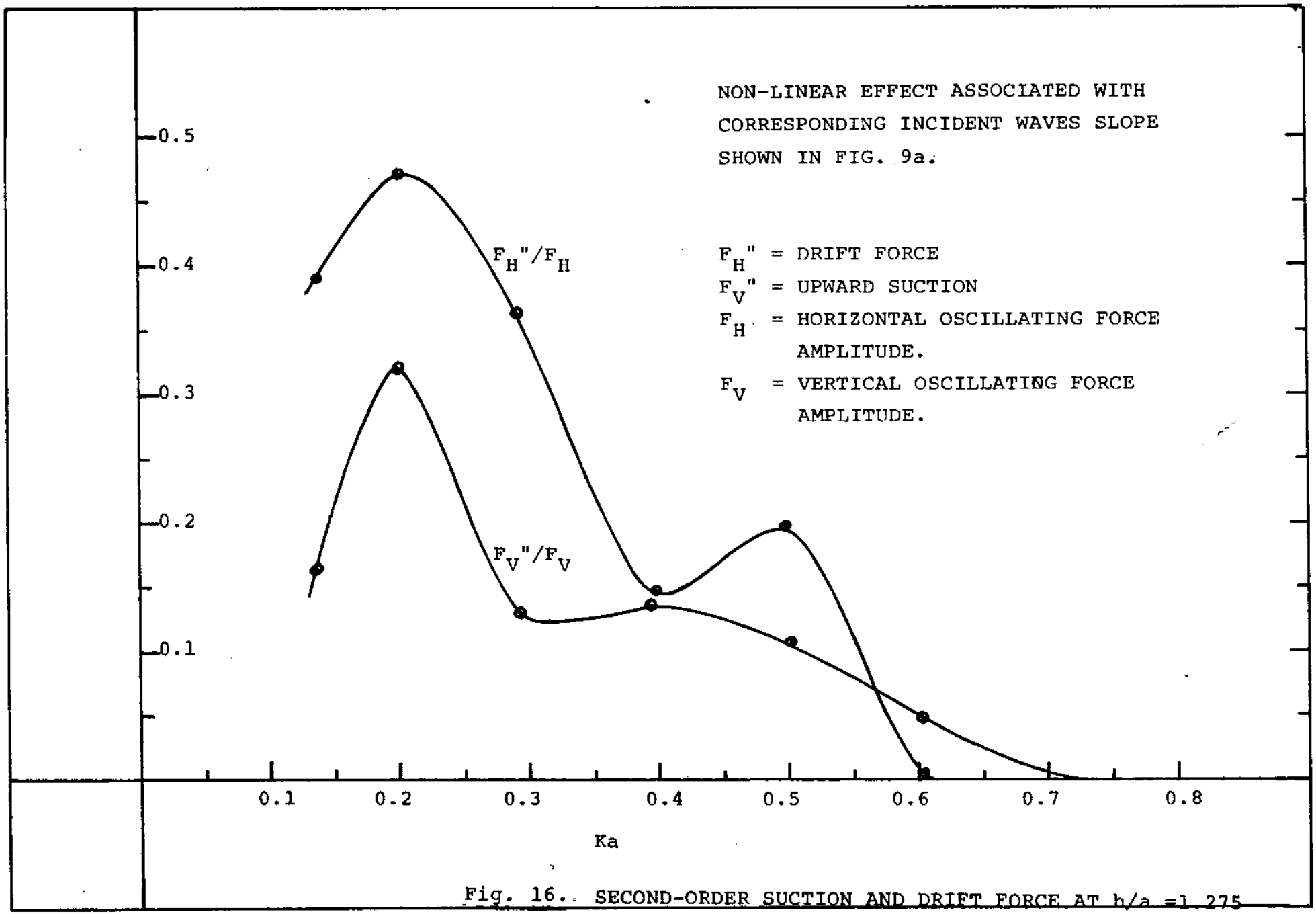

Fig. 16. SECOND-ORDER SUCTION AND DRIFT FORCE AT h/a =1.275

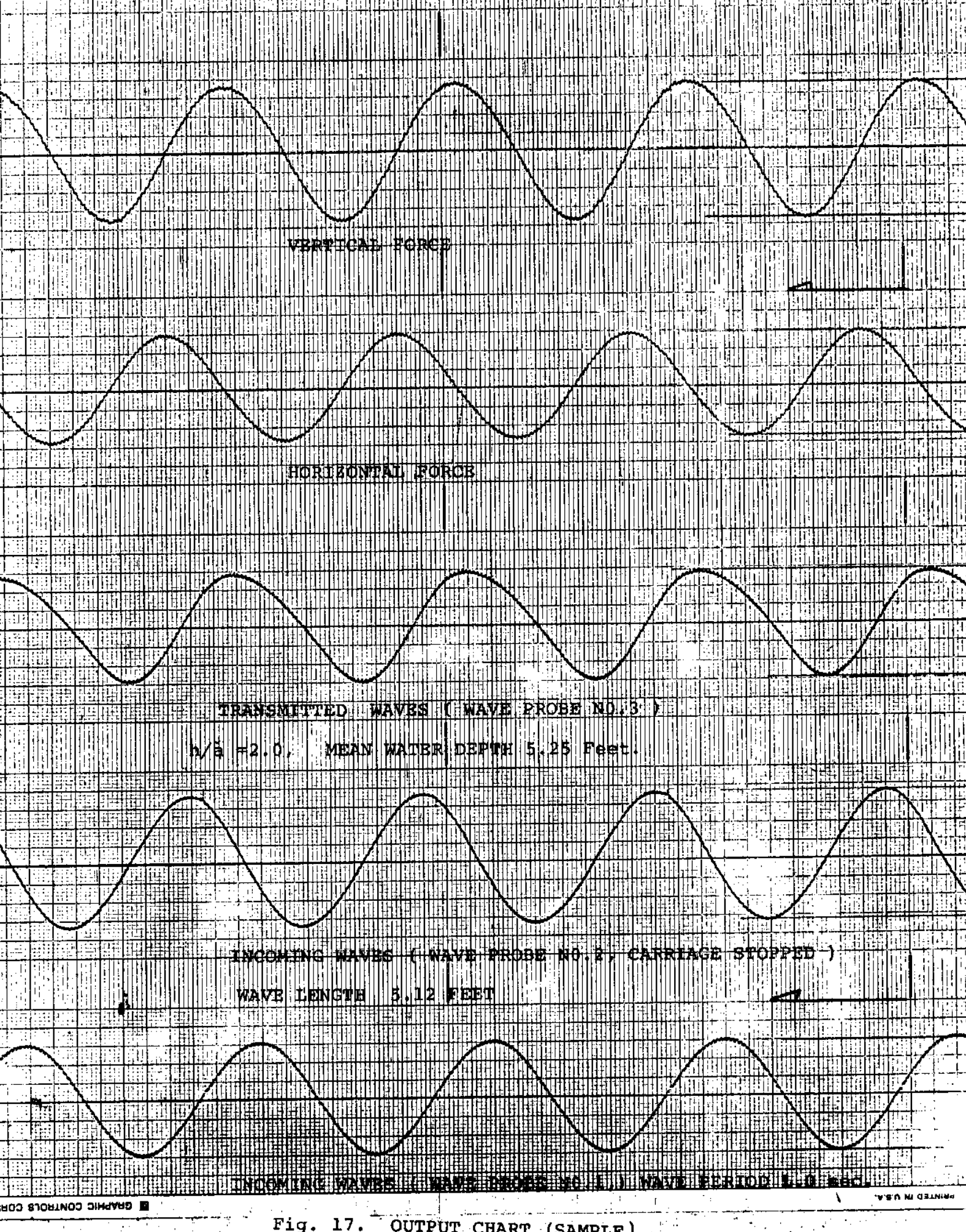

Fig. 17. OUTPUT CHART (SAMPLE)

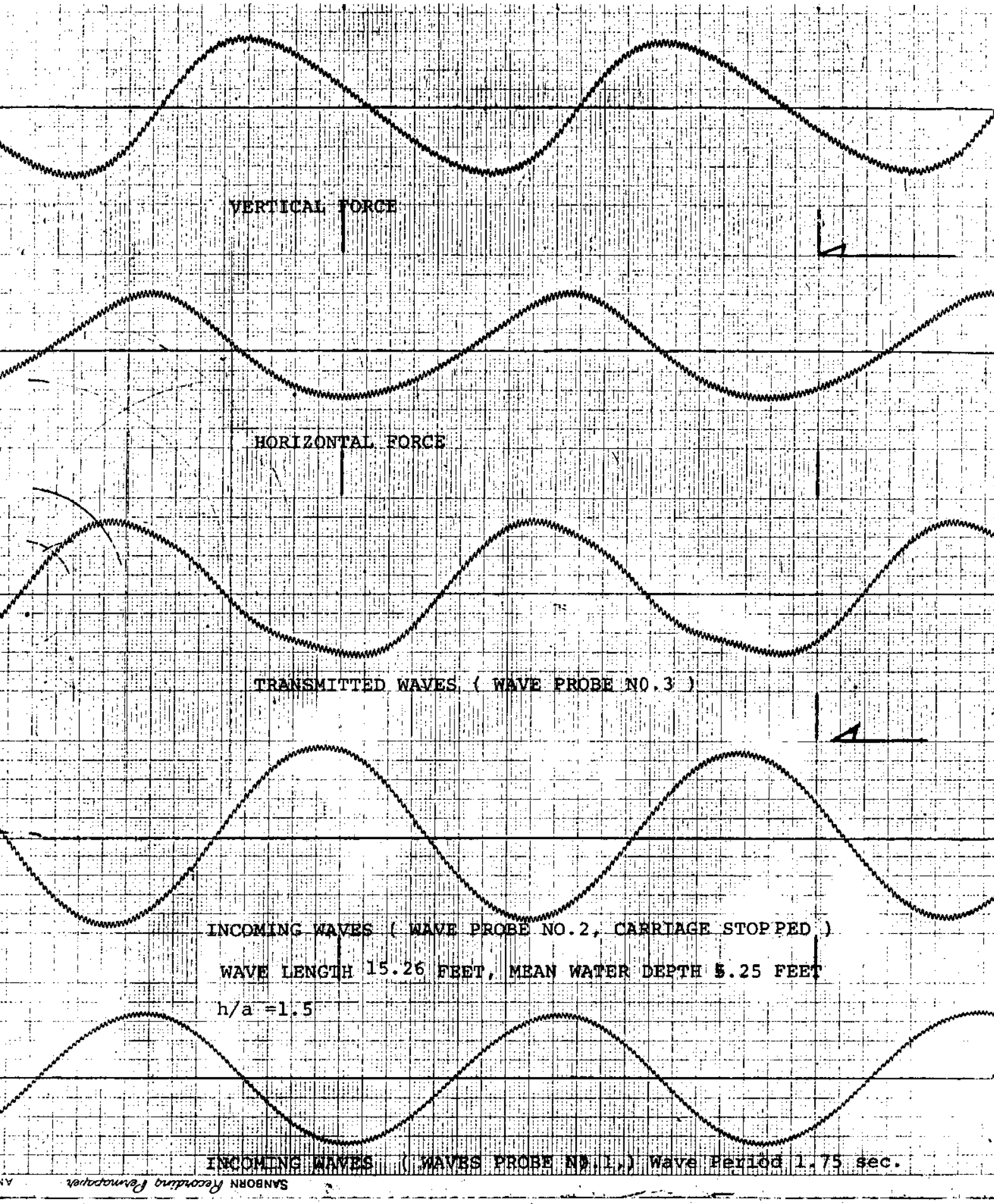

Fig. 18. OUTPUT CHART (SAMPLE)